Advanced Materials Research Vol. 936 (2014) pp 2054-2062
© (2014) Trans Tech Publications, Switzerland
doi:10.4028/www.scientific.net/AMR.936.2054

The Fracture Properties of Sandwich Structures Based on a Metal Foam Core

Yiou Shen[1, a], Yan Li[1,b], Wesley Cantwell [2,c] and Yuyuan Zhao[3,d]

[1] School of Aerospace Engineering and Applied Mechanics, Tongji University,

, Shanghai, 200092, P R China

[2]Department of Aerospace Engineering, Khalifa University of Science, Technology and Research (KUSTAR), PO. Box 127788, Abu Dhabi, UAE

[3]Department of Engineering, University of Liverpool, Liverpool, L69 3GH, UK

[a]syoeva@tongji.edu.cn, [b]liyan@tongji.edu.cn, [c]w.cantwell@liv.ac.uk, [d]y.y.zhao@liv.ac.uk

Keywords: Metal foam, sandwich structure, lost carbonate sintering, fracture

Abstract: The fracture properties of a series of metal foam sandwich structures based on glass fiber-reinforced polyamide 6,6 composite (GF/PA6,6) skins have been investigated. The open cell core materials were manufactured using the Lost Carbonate Sintering (LCS) process, a recently-developed technique for manufacturing metal foams. Initially, the effect of varying the compaction pressure used in producing the metal foams as well as the density of the samples were investigated through a series of compression tests. Here, it was shown that the compressive strength and the elastic modulus of the foams varied with density and compaction pressure, in spite of the fact that the average size of the cells in these foams were insensitive to either of these two parameters.
The resistance of sandwich structures to localized loading was investigated through a series of indentation tests. Here, it was shown that the indentation response of sandwich structures could be characterized using a simple indentation law, the parameters of which did not exhibit any clear dependency on the density of the foam. Finally, three point bend tests on the sandwich structures have shown that their loading-bearing properties were sensitive to foam density.

Introduction

Traditional fiber reinforced sandwich structures are based on polymer core materials, however, polymer foams typically offer a relatively low strength and only a moderate energy-absorbing capacity. Recently, a range of lightweight metallic core materials offering higher strength, stiffness and energy absorption characteristics have been developed for applications in the aerospace, land and marine sectors [1-5]. Currently, there are a number of processing technologies used in the manufacture of metal foams. Frequently, a liquid-state foaming route is employed for manufacturing low-melting-point metal systems such as aluminum foam [2]. In contrast, high-melting-point metal cores are usually manufactured by a solid state method such as a powder metallurgy process. However, many commercial aluminum foams offer cell sizes between 2 and 10 mm. Recently, the introduction of the Lost Carbonate Sintering (LCS) process has enabled researchers to manufacture open-cell metal foam structures with well-controlled cell dimensions at very low cost [6-13]. The work presented in this paper investigates the properties of a metal foam-based sandwich structure based on glass fiber-reinforced composite skins. Iron powder was employed to manufacture the metal foams via the LCS process. Iron foam offers several advantages over aluminum foam, including a higher strength and stiffness, lower raw material costs and a higher melting temperature [14]. Initially, the mechanical properties of the foam materials are investigated through a series of compression tests on cylindrical samples. Following this, the indentation and flexural properties of sandwich structures based on glass fiber reinforced polyamide 6,6 composite skins are investigated.

All rights reserved. No part of contents of this paper may be reproduced or transmitted in any form or by any means without the written permission of TTP, www.ttp.net. (ID: 138.253.116.216-21/05/14,11:08:39)

Experimental procedure

The iron foam cores investigated in this study were manufactured using the Lost Carbonate Sintering (LCS) process, a procedure that is described in detail elsewhere [7]. The raw materials used here were based on iron powder (supplied by Pometon Metal Powders), potassium carbonate (K_2CO_3) spheres (supplied by E&E Ltd in Widnes, UK) and glass fiber reinforced polyamide 6,6 (TEPEX) composite skins (supplied by Bond Laminates, Germany). The iron powder used in this study (FERSINT RI 180/3.0) was supplied with a particle size between 25 and 200 μm and the K_2CO_3 spheres used in the LCS process were in the size range of 710 to 1000 μm. The thickness of the glass fiber reinforced polyamide 6,6 composite used in the manufacture of the skins was 0.5 mm. The nominal volume fraction of iron in the Fe-K_2CO_3 mixtures was 0.25, 0.3 and 0.35, yielding metal foam samples with nominal relative densities of 0.2, 0.25 and 0.29, respectively. The Fe-K_2CO_3 mixtures were sealed in cylindrical mild steel tubes by placing iron powder in the two ends. The samples were compacted by a press prior to sintering. Three compaction pressures were used during the manufacture of the foam samples, these being 100, 150 and 200 MPa. Following compaction the samples were sintered in a temperature-controlled electrical furnace. The temperature in the furnace was increased at a rate of 10℃ per minute from room temperature to 850℃ and samples were sintered at this temperature for 4 hours. After the sintering process was complete, the K_2CO_3 particles were dissolved in running water for 90 minutes. The resulting metal foams were subsequently dried in an oven for two hours at a temperature of approximately 100℃. This process yielded high quality foams with an open-cell structure.

A series of mechanical tests were carried on foams manufactured using compaction pressures of 100, 150 and 200 MPa. The iron foam specimens used in these compression tests were based on 20 mm diameter, 10 mm high cylinders. The compression tests were carried out on an Instron 4505 universal test machine at a crosshead displacement rate of 1 mm/min. Following the compression tests on the plain iron foam samples, a series of sandwich structures were manufactured to evaluate the potential offered by such core materials. Here, an Araldite LY5082 epoxy resin combined with an Araldite AY 103 hardener was used to bond the core and glass fiber/polyamide 6,6 skin materials. After the resin was applied, the sandwich beams were placed under a light pressure and left overnight at room temperature to ensure complete curing of the adhesive. Initially, indentation tests were conducted on sandwich beams positioned on a solid base. Samples with dimensions of 120 x 25 x 25 mm (manufactured using a compaction pressure of 100 MPa) were tested on an Instron 4505 mechanical test machine at a crosshead displacement rate of 1 mm/min. The diameter of the indentor was 10 mm and the maximum indentation was approximately one millimeter. Three point bend tests were conducted on samples with dimensions of 120 x 25 x 25mm (a compaction pressure of 100 MPa was used due to limitations in the capacity of the press) on an Instron 4505 universal test machine. The beams were supported on two 10 mm diameter cylinders positioned 100 mm apart. A 10 mm diameter steel indentor was used to load the samples at a crosshead displacement rate of 1 mm/minute.

Results and Discussion

Compressive properties of the core materials

Fig. 1 shows the microstructures of the three densities of iron foam manufactured using compaction pressure of 200 MPa. Fig. 1a, the sample with a relative density of 0.2 indicates that many of the cell walls have not fully formed during the sintering process and a number of cell walls have fractured, possibly during the subsequent grinding process. The microstructures of the foams with relative densities of 0.25 and 0.29, Figs. 1b and 1c, are better defined, with the individual cells being more clearly visible. Closer examination highlights the fact that some cells here effectively merged and the cell wall is missing. This occurs when two potassium carbonate particles are in very close proximity and the metal powder is forced out. The average diameters of cells in the three foams were measured and Fig. 1 shows the variation of the average cell diameter with relative density. Clearly, the

average cell sizes in the three types of foam are similar suggesting that the size of the cells does not vary over the range of densities considered. It is evident from the micrographs and the data in Fig. 1 that the average cell size reflects the size of the potassium carbonate particles used in the manufacture of the foams. Fig. 2 shows the variation of cell size with compaction pressure where it is again evident that the size does not vary over the range of manufacturing conditions studied here. The degree of voiding in the cell walls decreased as the compaction pressure was increased, indicating that the higher manufacturing pressures produced a greater level of contact during the sintering stage. Clearly, the size of the cells in these systems is significantly smaller than those observed in commercially available metal forms where values in the latter can be as large as 10 mm [15].

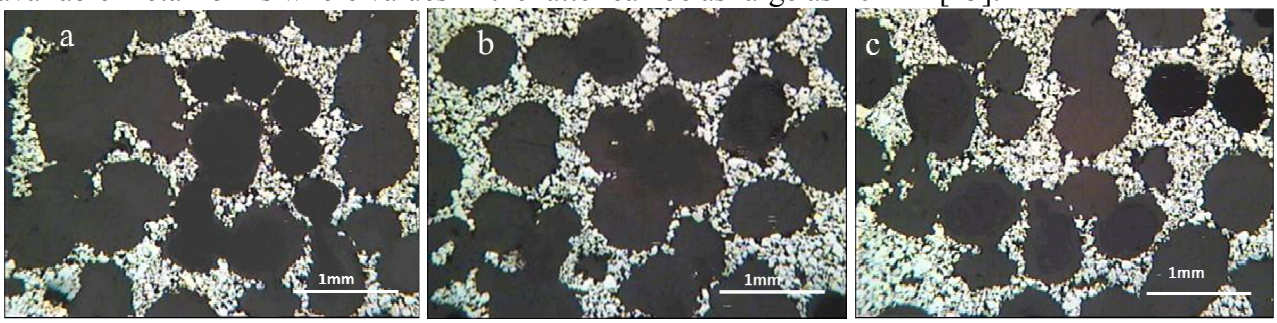

Fig. 1 Microstructure of the foam cell, (a) relative density of the foam was 0.20, (b) relative density of the foam was 0.25, (c) relative density of the foam was 0.29.

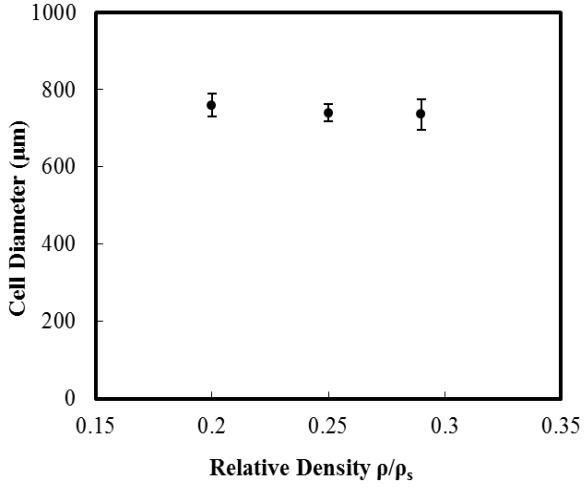

Fig. 2 The variation of cell diameter with relative density for foams manufactured using a compaction pressure of 200 MPa.

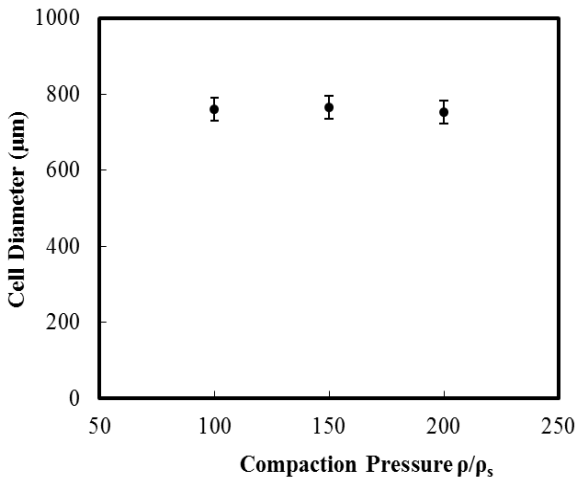

Fig. 3 The variation of cell diameter with compaction pressure for foams with a relative density of 0.25.

Fig. 4 shows typical stress-strain traces following compression tests on samples manufactured using compaction pressures of 100, 150 and 200 MPa. In each case, the relative density of foams was nominally 0.25. The curves in Fig. 4 exhibit a region of linear elasticity at low stresses, followed by a long plateau stress before the stress rises steeply in the regime of densification. Included in the stress-strain trace for the 200 MPa sample is the procedure for determining the plastic collapse stress, σ_{pl}. The figure shows that increasing the compaction pressure serves to increase both the plastic collapse stress and the stress at the onset of densification (the final rise in the stress-strain plot). Fig. 5 shows sections removed from samples that had been subjected to strains ranging from 0.2 to 0.5. An examination of the micrographs indicates that the samples fail due to the cell wall buckling and collapse under the increasing strain. At a strain of 0.2, Fig. 5a, a number of cell walls close to the top of the sample fail causing strain localization. With increasing strain, the regions in which cell wall buckling occurs increase in size, spreading out across the sample. At a strain of 0.5, Fig. 5d, virtually all of the cell walls have collapsed and densification occurs. Fig. 6 shows the variation of the plastic collapse stress of the foams, σ_{pl}, with compaction pressure. Clearly, the plastic collapse stress

increases rapidly with the level of pressure applied during compaction, indicating that this processing parameter has a significant effect on the mechanical properties of the foam. As previously stated, increasing the compaction pressure forces the metal particles into contact during the sintering process, leading to fewer voids in the cell walls following manufacture.

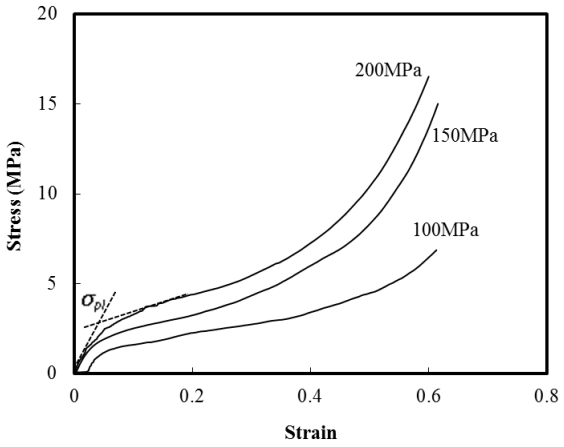

Fig. 4 Typical stress-strain curves following compression tests on samples manufactured using compaction pressures of 100, 150 and 200 MPa. The relative density of the foam was 0.25.

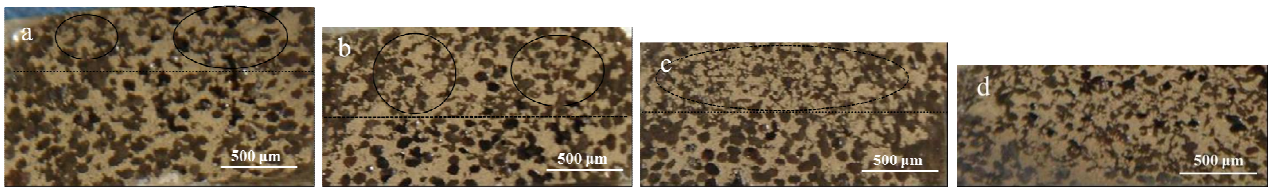

Fig. 5 Deformation banding during a typical compression test: (a) ε=0.2, (b) ε=0.3, (c) ε= 0.4, (d) ε=0.5.

Fig. 7 shows typical compression stress-strain curves following tests on the three different densities (0.20, 0.25 and 0.29) of metal foam manufactured using a compaction pressure of 200 MPa. It is clear from Fig. 7 that the stress-strain response of the foam samples depends on the density of iron foam; this phenomenon was also observed by Park et al [14]. Lowering the density of the foam gives a more pronounced plateau since the structure affords more opportunity for cell walls to deform and collapse during the loading process. The variation of the plastic collapse stress with relative density is shown in Fig. 8. Clearly, the compressive properties of the foam increases rapidly with foam density. The compressive properties of these foams compare favourably with previously published data for an aluminum foam where values of compression strength of approximately 1.5 MPa were recorded [15].

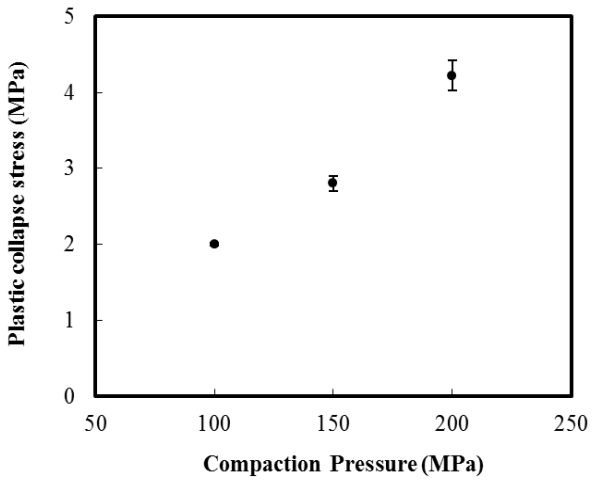

Fig. 6 The variation of compressive stress with compaction pressure. The relative density of the foam was 0.25.

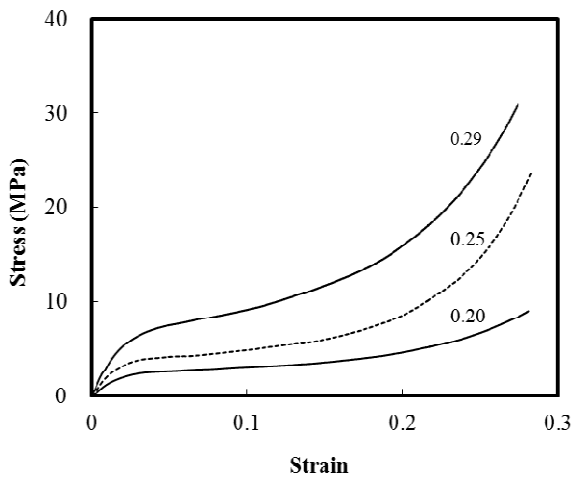

Fig. 7 Typical stress-strain curves following compression tests on samples manufactured using a compaction pressure of 200 MPa.

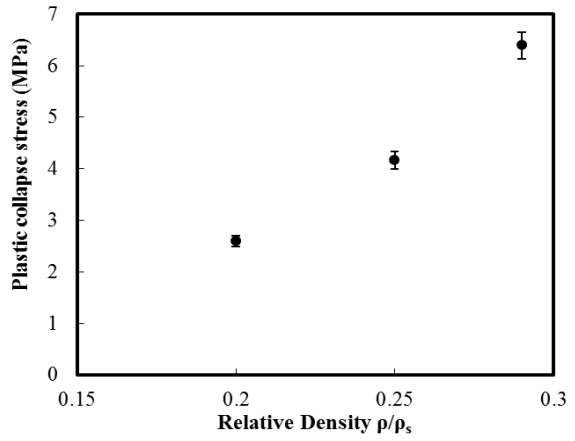

Fig. 8 The variation of compressive stress with relative density for foams manufactured using a compaction pressure of 200 MPa.

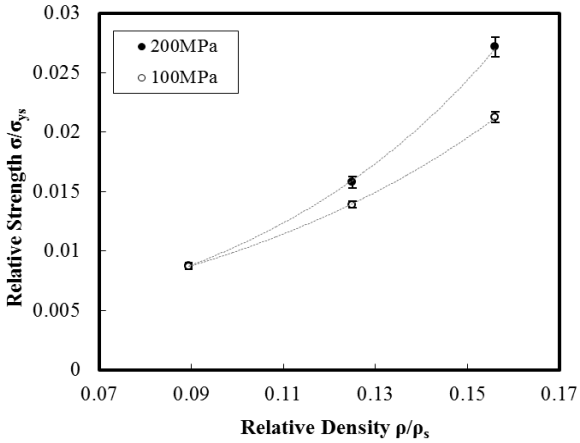

Fig. 9 The variation of relative strength with relative density for foams manufactured using compaction pressures of 100 MPa and 200 MPa.

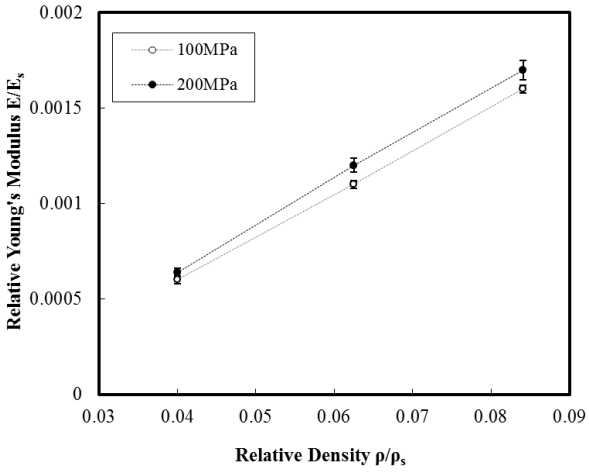

Fig. 10 The variation of the relative Young's modulus with relative density for foams manufactured using compaction pressures of 100 MPa and 200 MPa.

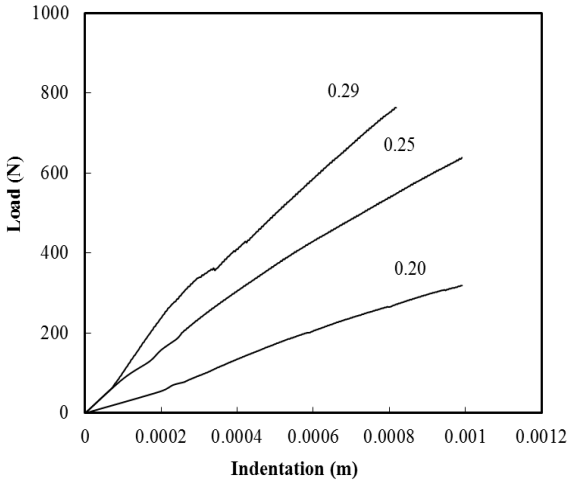

Fig. 11 Typical load-indentation curves for the sandwich structures manufactured using a compaction pressure of 100 MPa.

Table 1 summarises the average plastic collapse stresses of the foams considered here. Clearly, the plastic collapse stress of the foam is sensitive to both density and compaction pressure. The strength data for the iron foam are plotted as a function of relative density in Fig. 9. Previous work [3] investigating the compressive properties of open-cell foam structures has shown that the relative plastic-collapse stress, σ_{ys}, of such a structure can be written in the form:

$$\frac{\sigma_{pl}}{\sigma_{ys}} = \mathrm{M}\left(\frac{\rho}{\rho_s}\right)^{3/2} \tag{1}$$

where ρ/ρ_s is the relative density, σ_{ys} is the yield strength of the solid material and M is a constant with a value equal to approximately 0.3 [3]. In this study, the data from the compression tests were forced to fit this type of relationship, yielding a value for M. The data in Fig. 10 were used to determine the appropriate values of M in Equation 1. Table 2 summarizes the average values of M where it can be seen that the experimentally-determined values are well below the values of 0.3 predicted by a cubic model for open-cell foams [3]. Since the model assumes a cubic cell geometry and the iron foams are clearly more irregular than this, some significant deviation between the measured and predicted behavior is expected.

TABLE 1 SUMMARY OF THE PLASTIC COLLAPSE STRESSES OF THE METAL FOAMS.

Relative density	Compaction Pressure (MPa)		
	200 MPa	150MPa	100 MPa
0.20	2.18		
0.25	4.30	2.80	2.00
0.29	7.24		

TABLE 2 SUMMARY OF THE CONTACT PROPERTIES OF THE METAL FOAMS [3].

	Theoretical value	Compaction Pressure (MPa)	
		100	200
M	0.3	0.144	0.174
C	1	0.018	0.018

The relative Young's modulus properties of the foams are summarized in Fig. 10. Previous work has shown that the relative Young's modulus of a foam, E/E_s, (where E_s is the Young's modulus of the solid material) can be written in terms of its relative density, ρ/ρ_s, as follows [3]:

$$\frac{E}{E_s} = C\left(\frac{\rho}{\rho_s}\right)^2 \tag{2}$$

where C is a constant (approximately equal to unity for an open cell foam [3]). As before, this relationship was applied to the experimental data, yielding a value for the constant C. Table 2 reports the values of C for the systems evaluated here. It is clear that the measured values for this constant are significantly lower than those predicted by the cubic cell geometry.

Indentation characteristics of the sandwich structures

Fig. 11 shows typical load-indentations plots following tests on the three sandwiches manufactured using a compaction pressure of 100 MPa. Clearly, the slope of the load-indentation trace increases with foam density. It can be seen from the figure that the initial portions of the curves were slightly non-linear, and effect that may be due to the compliance of the test machine and a slight lack of fit in the test fixture. The reason for the change of slope in the sandwich structures was explained by Davies et al [16], who attributed it to the initiation of local damage such as core crushing under the point of indentation. The load, P, versus indentation, α, plots were forced to fit a generalized contact law of the form:

$$P = C\alpha^n \tag{3}$$

where n and C are indentation parameters that can be determined from the load-indentation plots. The type of relationship has been successfully used in previous studies investigating the indentation response of sandwich structures [17] and was considered appropriate here. Plots of *log P* versus log α were drawn, to yield the indentation parameter 'n' (from the slope of the graph) and the constant '*C*' (from the intercept with the y-axis).The values of the parameters *n* and *C* in this indentation law are summarized in Table 3, which dictate the shape and slope of the indentation trace [17]. The load-indentation curve should be a straight line when n is equal to unity, the curve will tend upwards when n is greater than one and downwards when n less than one. The value of *C* determines the effective gradient of the curve.

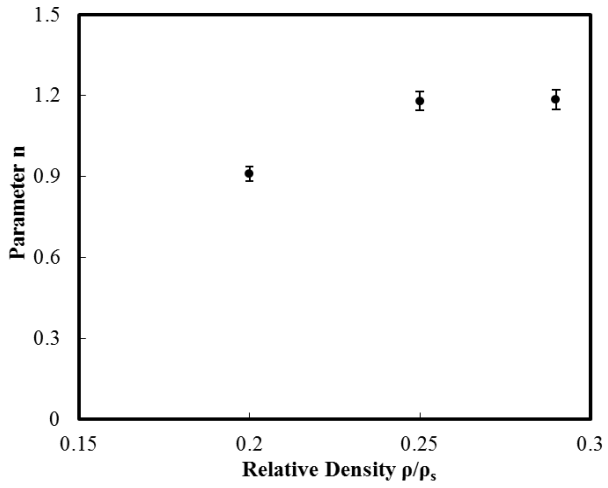

Fig. 12 The variation of the contact parameter, n, with relative density for foams manufactured using a compaction pressure of 100 MPa.

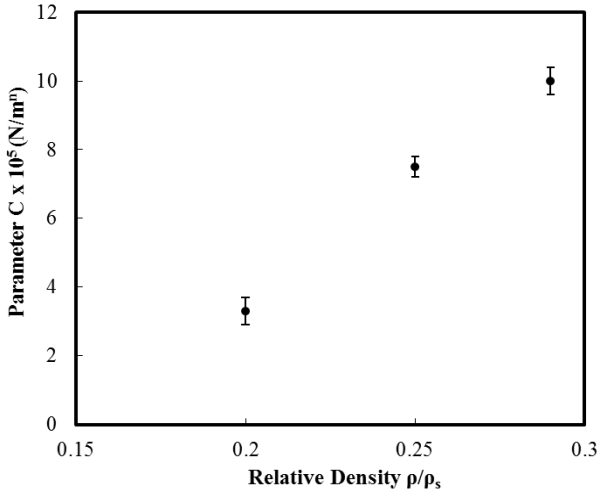

Fig. 13 The variation of the contact parameter, C, with relative density for foams manufactured using a compaction pressure of 100MPa.

TABLE 3 SUMMARY OF THE CONTACT PROPERTIES OF THE SANDWICH STRUCTURES FOLLOWING INDENTATION TESTS.

Relative Density	C (N/m^n)	n
0.2	3.3×10^5	0.91
0.25	7.5×10^5	1.18
0.29	1.0×10^6	1.185

The variation of the parameter 'n' with relative density is shown in Fig. 12; the average values of 'n' for the 100 MPa samples varied between 0.91 and 1.185. It can be seen that for the samples with a relative density of 0.2, the average values of 'n' are lower than unity, approximately 0.91. In contrast, samples with relative densities of 0.25 and 0.29, the average values are clearly greater than unity. Similar results were observed when the parameter 'C' is plotted against relative density as shown in Fig. 13. The average values of 'C' show an increasing trend with increasing relative density. This is expected since increasing the density of the foam increases the stiffness of the sandwich structure, thereby increasing the effective slope of the load vs. indentation curve.

Flexural properties of the sandwich structures

Fig. 14 shows typical load-displacement curves following three-point bending tests on the sandwich structures. Fig. 15 shows a photograph of a fractured sandwich structure following a three-point bend test, the relative density of the foam in this sample was 0.25. From the figure, it can be seen that the core has fractured in shear at one end of the sample leading to debonding of the composite skin along the uppermost interface. Similar failure modes were observed in the samples based on foams with relative densities of 0.2 and 0.29. Clearly, the load-bearing capacity of the sandwich structures is limited by the fracture properties of the core. Similar modes of failure have been observed following three-point bend tests on aluminum foam core sandwich structures based on glass fiber PA 6,6 skins [15].The maximum stress in the lower composite skin at maximum load was determined using sandwich beam theory. Here, the maximum tensile stress in the lower face is given as:

$$\left(\sigma_f\right)_{\max} = \pm \frac{ME_f}{D}\frac{h}{2} \tag{4}$$

where M is the maximum bending moment, E_f is the modulus of the composite skins and D can be approximated as [1]:

$$D = E_f \frac{btd^2}{2} \tag{5}$$

where the dimensions b, t and d are defined in Fig. 16.

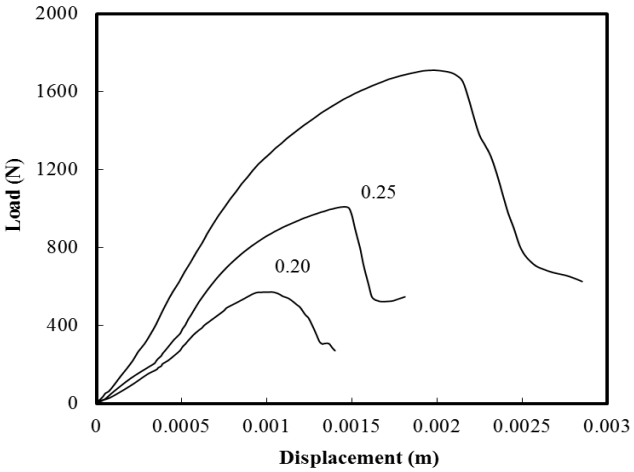

Fig. 14 Typical load-displacement curves following three point bend tests on sandwich structures manufactured using a compaction pressure of 100 MPa.

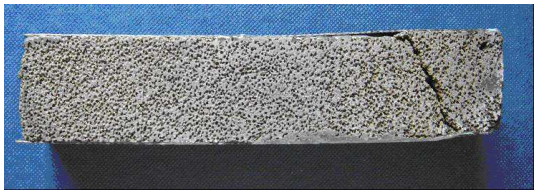

Fig. 15 The photograph of deformed sandwich structure after three point bend testing, relative density of foam was 0.25.

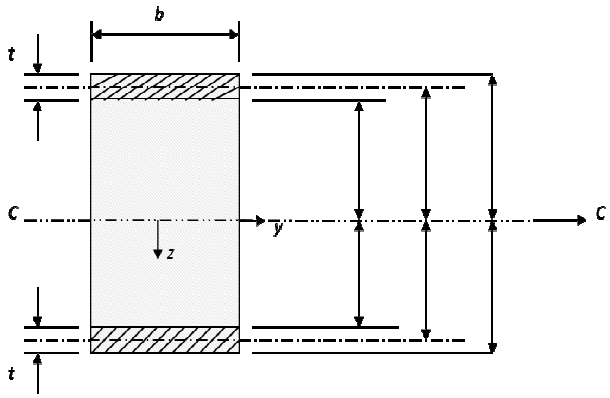

Fig. 16 Schematic of the cross-section of a sandwich beam showing the characteristic dimensions.

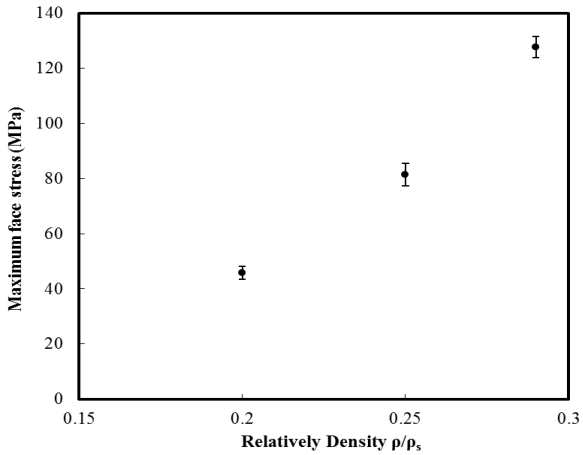

Fig. 17 The variation of the face stress with relative density for sandwich structures manufactured using a compaction pressure of 100 MPa.

The average values of the maximum stress in the face material were calculated using Eqn. 4 and these values are shown in Fig. 17. From the figure, it is clear that the stress in the lower skin at failure increases as the relative density increases. The maximum stress in the skins in the highest density laminate was approximately 130 MPa, this being approximately thirty percent of the tensile strength of the composite skins. Clearly, the strength of the sandwich structures is limited by the shear strength of the core, increasing as the shear strength of the core increases. These findings do suggest, however, that the LCS technique offers potential for manufacturing low cost metal foam cores for use in the manufacture of sandwich structures. The LCS technique is currently being used to manufacture metal cores based on other metal alloys such as steel and nickel-titanium shape memory alloys.

Summary

A range of iron foam core sandwich structures have been manufactured by the LCS process. Initial tests to characterize the mechanical properties of core materials have shown that the compressive strength and the elastic modulus of the systems were sensitive to the relative density of the foam and the compaction pressure used during manufacture. The compressive strength of the foams was also sensitive to the geometry of the foam.

Indentation tests on the sandwich structures have shown that the load-indentation response of these systems can be characterized using a generalized indentation law. Subsequent three point bend tests have shown that the load-bearing properties of these systems are also sensitive to the relative density of the core.

References

[1] Allen H.G., Analysis and Design of Structural Sandwich Panels, Pergamon, London, 1969.

[2] Ashby M.F., Evans A.G., Fleck N.A., Gibson L.J., Hutchinson J.W. and Wadley H.N.G, Metal Foams: A Design Guide. Boston: Butterworth-Heinemann; 2000.

[3] Gibson L.J. and Ashby M.F., Cellular Solids: Structure and Properties, 2nd Ed., Cambridge University Press, Cambridge, 1997.

[4] Banhart J., Ashby M. and Fleck N., Cellular Metals and Metal Foaming Technology, MIT-Verlag, Berlin 2001.

[5] Lenel Fritz V, Powder Metallurgy: Principles and applications, Metal Powder Industries Federation, Princeton (N.J.), 1980.

[6] Zhao Y.Y., Porous metallic materials and method of production thereof, UK Patent Application Number: 0412125.7, 2004.

[7] Zhao Y.Y., Fung T., Zhang L.P., and Zhang F.L., Lost carbonate sintering process for manufacturing metal foams, Scripta Materialia, 52(2005) 295-298.

[8] Zhao Y.Y. and Sun D.X., A novel sintering-dissolution process for manufacturing Al foams, Scripta Materialia, 46(2001), 273-282.

[9] Sun D.X., and Zhao Y.Y., Static and dynamic energy absorption of Al foams produced by the sintering and dissolution process, Metallurgical and Materials Transactions B, 34(2003), 69-74.

[10] Zhao Y.Y., Stochastic modelling of removability of NaCl in sintering and dissolution process to produce Al foams, Journal of Porous Materials, 10(2003), 105-111.

[11] Zhao Y.Y., Han F.S. and Fung T., Optimisation of compaction and liquid-state sintering in sintering and dissolution process for manufacturing Al foams, Materials Science and Engineering A, 364(2004), 118-126

[12] Sun D.X. and Zhao Y.Y., Phase changes in sintering of Al/Mg/NaCl compacts for manufacturing Al foams by the sintering and dissolution process, Materials Letters, 59(2005) 6-10.

[13] Ma X., Peyton A.J. and Zhao Y.Y., Measurement of the electrical conductivity of open-celled aluminium foam using non-contact eddy current techniques, NDT & E International, 38(2005) 295-298.

[14] Park C., Nutt S. R., PM Synthesis and properties of steel foams, Materials Science and Engineering, A288 (2000) 111-118.

[15] Kiratasaevee H., PhD thesis, the University of Liverpool, 2004.

[16] Davies P., Choqueuse D. and Wahab A., Response of composite sandwich panels to impact loading, Revue de l' Institut, Francais du Petrole, 1995.

[17] Hazizan M. K., Cantwell W. J., The low velocity impact response of foam-based sandwich, structures, Composites: Part B 33(2002) 193-204.